Cellular and Metabolic Profiling the Tumor-Stroma Interface via High-Dimensional Spatial Proteomics and Image Analysis (ESSB 2026)

Arutha Kulasinghe[1], Felicia Roland[2], Michelle Poulin[2], Ritu Mihani[2], Katherine Hales[3], Daniel Winkowski[3]

(1) Frazer Institute, University of Queensland (2) Akoya Biosciences, a Quanterix Company, Marlborough, MA, (3) Visiopharm Corp., Broomfield, CO.

Abstract

There remains a critical need for robust prognostic and predictive biomarkers to improve patient stratification for cancer immunotherapy across solid tumors. The tumour microenvironment (TME), particularly the tumour–stroma interface, is increasingly recognized as a potentially key determinant of therapeutic response, yet remains insufficiently characterized. In this study, we leveraged high-dimensional spatial proteomics combined with advanced image analytics to interrogate the cellular, functional, and metabolic architecture of tumour, stromal, and interface regions, with a focus on biologically active transition zones.

Using the Phenocycler-Fusion 2.0 platform with a custom immuno-metabolic panel targeting over 68 proteins, we profiled markers spanning tumour identity, stromal structure, immune cell subsets, functional states, and metabolic activity. This enabled high-resolution mapping of cell types, subtypes, and metabolic phenotypes across spatially defined compartments. Advanced image analysis via Visiopharm's pipeline facilitated accurate segmentation of tumour cores, stromal regions, and interface zones, while a Phenoplex™-guided workflow supported integrated cellular and metabolic characterization.

Our findings demonstrate that tumour and stromal core regions are both compositionally and metabolically distinct from their respective interface regions. While overall cellular proportions alone were not predictive of clinical outcomes, deeper analysis of functional and metabolic heterogeneity revealed important insights. Notably, we identified a tumour-specific metabolic signature associated with poorer clinical outcomes. In contrast, increased metabolic activity in immune cells localized to the tumour–stroma interface was associated with improved responses to immunotherapy, suggesting that spatially resolved immune fitness plays a central role in driving benefit.

Collectively, these results highlight the importance of integrating spatial proteomics with advanced image analytics to uncover biologically meaningful features of the TME. This approach provides a powerful framework for identifying novel biomarkers and improving our understanding of the mechanisms governing response to immunotherapy.

Results – Compositional differences between Primary and Metastatic TNBC

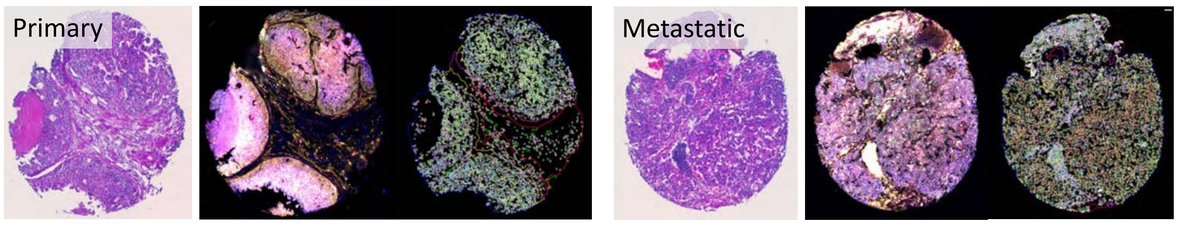

Figure 2. Representative H&E and mIF cores of TNBC TMA with annotated regions of interest (ROI).

	L-AF750 (AF 750)	)-AF750 (AF 750)	(TTO550 (ATTO 55	3e-AF647 (Cy5) (M	4-AF647 (Cy5) (M	TTO550 (ATTO 55	36-AF647 (Cy5) (M	38-AF647 (Cy5) (M	ITO550 (ATTO 55(	-ATTO550 (ATTO	P3-AF647 (Cy5) (I	)-AF750 (AF 750) (	1-AF750 (AF 750)	3-ATTO550 (ATTO	ITO550 (ATTO 55(	K-AF750 (AF 750)
Total	22894	22662	4045	34243	27712	37471	1276	20454	10376	8561	6984	16242	45949	2090	6693	42749
BCLXL-AF750 (AF 750) (MFI)	22894	782	2217	1559	4507	2146	314	2771	1248	5195	1508	5987	8701	210	2930	18370
CD20-AF750 (AF 750) (MFI)	782	22662	1405	12873	9285	18897	156	4464	2371	221	1417	2112	12464	422	826	874
CD21-ATTO550 (ATTO 550) (MFI)	2217	1405	4045	620	1537	1248	214	112	216	2064	607	2649	3725	6	1010	2801
CD3e-AF647 (Cy5) (MFI)	1559	12873	620	34243	19974	26722	172	8589	9461	178	3755	2539	17998	1199	853	1656
CD4-AF647 (Cy5) (MFI)	4507	9285	1537	19974	27712	20917	335	9536	4422	1518	4085	3275	17118	1083	2254	4578
CD45-ATTO550 (ATTO 550) (MFI)	2146	18897	1248	26722	20917	37471	306	12473	8432	173	4542	4092	21918	1370	1000	1779
CD56-AF647 (Cy5) (MFI)	314	156	214	172	335	306	1276	192	96	263	149	268	1051	18	157	935
CD68-AF647 (Cy5) (MFI)	2771	4464	112	8589	9536	12473	192	20454	3724	200	3609	3078	11291	983	652	1900
CD8-ATTO550 (ATTO 550) (MFI)	1248	2371	216	9461	4422	8432	96	3724	10376	178	1031	1472	5947	811	384	1218
Ecadherin-ATTO550 (ATTO 550) (MFI)	5195	221	2064	178	1518	173	263	200	178	8561	470	4546	5924	34	1402	8328
FOXP3-AF647 (Cy5) (MFI)	1508	1417	607	3755	4085	4542	149	3609	1031	470	6984	1953	4455	170	942	1454
G6PD-AF750 (AF 750) (MFI)	5987	2112	2649	2539	3275	4092	268	3078	1472	4546	1953	16242	9523	337	1737	11806
GLUT1-AF750 (AF 750) (MFI)	8701	12464	3725	17998	17118	21918	1051	11291	5947	5924	4455	9523	45949	906	3567	16333
GranzymeB-ATTO550 (ATTO 550) (MFI)	210	422	6	1199	1083	1370	18	983	811	34	170	337	906	2090	47	512
Ki67-ATTO550 (ATTO 550) (MFI)	2930	826	1010	853	2254	1000	157	652	384	1402	942	1737	3567	47	6693	5218
PanCK-AF750 (AF 750) (MFI)	18370	874	2801	1656	4578	1779	935	1900	1218	8328	1454	11806	16333	512	5216	42749

Figure 3. Co-Localization Matrix shows cellular co-expression of biomarkers across the TME to validate accurate thresholding and increase confidence in phenotype outputs.

Figure 4. t-SNE maps of the cellular composition in the tumour (top) and stromal (bottom) regions between primary and metastatic TNBC

Results – TIL scoring

Figure 5. Immune cell scoring across each core for CD8, CD4, CD56, CD20, and across the tumor, stroma and margin regions.

Methods

CoRegistration → Map Tissue → Segment Cells → Phenotype

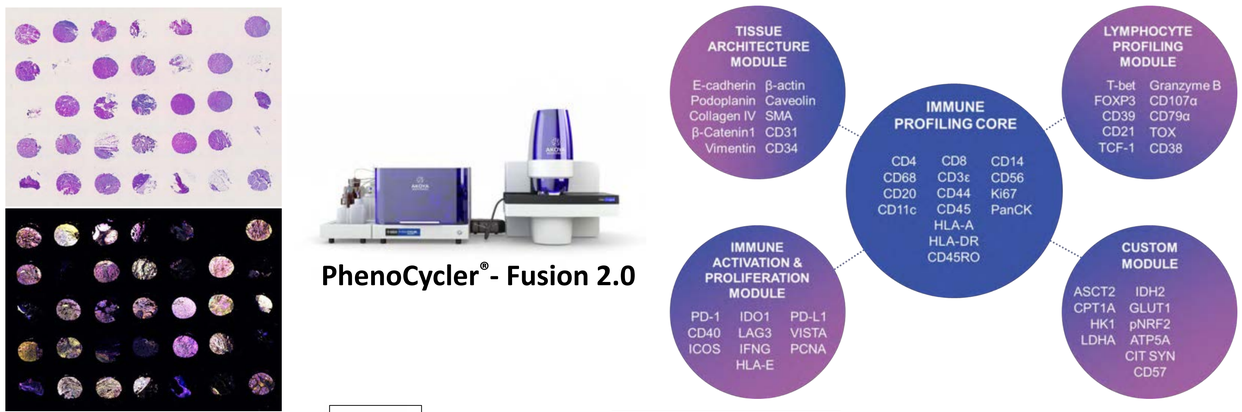

Figure 1. H&E and representative mIF cores of TNBC tissue microarray (TMA), biomarker panel on PCF, and Phenoplex workflow.

Results – Metabolic scoring

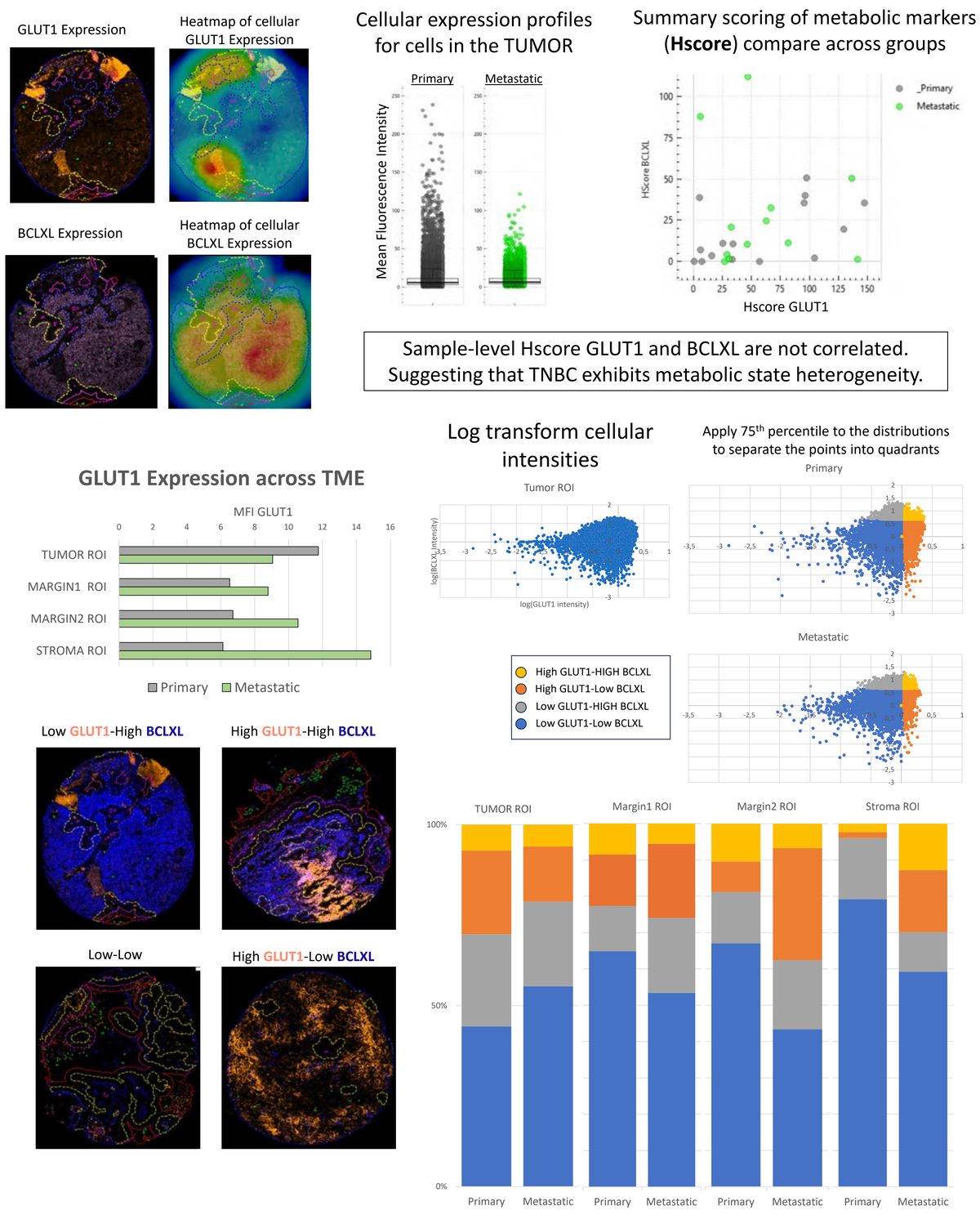

Figure 6. Framework for metabolic marker scoring across the TME landscape.

Conclusions

This study highlights the framework for ultrahigh-plex discovery spatial proteomic profiling and image quantification in TNBC. Most notably, the modular analysis capability highlights how features of importance can be analysed (composition, TIL and metabolic scoring). Most notably, the metabolic scoring could be developed into a "H-score" enabling quantification of this signal to aid in functional cell phenotyping.